New simple panchromatic dyes based on thiadiazolo[3,4-c]pyridine unit for dye-sensitized solar cells

Article *in* Dyes and Pigments · March 2014

DOI: 10.1016/j.dyepig.2013.11.001

Dyes and Pigments 102 (2014) 196–203

Contents lists available at ScienceDirect

Dyes and Pigments

journal homepage: www.elsevier.com/locate/dyepig

New simple panchromatic dyes based on thiadiazolo[3,4-*c*]pyridine unit for dye-sensitized solar cells

Yong Hua [a,b,1], Hongda Wang [a,1], Xunjin Zhu [a,b,*], Ashraful Islam [c,2], Liyuan Han [c,2], Chuanjiang Qin [c,**], Wai-Yeung Wong [a,b,*], Wai-Kwok Wong [a,b,*]

[a] Department of Chemistry and Institute of Molecular Functional Materials, Hong Kong Baptist University, Waterloo Road, Kowloon Tong, Hong Kong, China
[b] Changshu Research Institute of Hong Kong Baptist University, Changshu, Jiangsu Province 215500, PR China
[c] Photovoltaic Materials Unit, National Institute for Materials Science, Sengen 1-2-1, Tsukuba, Ibaraki, Japan

ARTICLE INFO

Article history:
Received 4 September 2013
Received in revised form
30 October 2013
Accepted 3 November 2013
Available online 13 November 2013

Keywords:
Thiadiazolo[3,4-*c*]pyridine
Electron-withdrawing
Triarylamine
Photosensitizer
Dye-sensitized solar cells
Panchromatic

ABSTRACT

Three new organic D–A–π–A photosensitizers with thiadiazolo[3,4-*c*]pyridine moiety incorporated between non-planar triarylamine and cyanoacrylic acid, have been developed and applied in dye-sensitized solar cells. It has been demonstrated that the incorporation of electron-withdrawing thiadiazolo[3,4-*c*]pyridine unit can effectively tune the HOMO and LUMO energy levels, extending the absorption spectra into the deep-red region and covering the whole visible region. The photoresponse of the cells based on the three dyes reached above 800 nm, a value which is comparable to the incident photon-to-current conversion efficiency onset of the established dye N719. Typically, three different bulky electron-donating units such as triphenylamine, *N*,*N*-bis(9,9-dimethylfluoren-2-yl)aniline and 4-(hexyloxy)-*N*-(4-(hexyloxy)phenyl)-*N*-phenylaniline were utilized to investigate their influences on the photovoltaic performances of DSSCs. The results indicate that the introduction of the strongest electron-donating 4-(hexyloxy)-*N*-(4-(hexyloxy)phenyl)-*N*-phenylaniline unit can further red-shift the intramolecular charge transfer band and enhance the light-harvesting properties, as well as retard the electron recombination between electrons at the TiO_2 and oxidized species of dye or I_3^- in the electrolyte. Under simulated AM 1.5G irradiation, the cell based on the dye derived from 4-(hexyloxy)-*N*-(4-(hexyloxy) phenyl)-*N*-phenylaniline produced a short-circuit photocurrent of 14.19 mA cm^{-2}, an open-circuit photovoltage of 0.462 V, a fill factor of 0.64, corresponding to a power conversion efficiency of 4.20%. Though the power conversion efficiency is still low, the methodology of tuning the HOMO and LUMO energy levels by incorporation of an electron-withdrawing thiadiazolo[3,4-*c*]pyridine unit in such D–A–π–A dyes could be generally applied to design more efficient panchromatic sensitizers in DSSCs.

1. Introduction

Dye-sensitized solar cells (DSSCs), referred to as one promising alternative to conventional semiconductor silicon-based solar cells, have been pioneered by Grätzel and co-workers in the last decade [1]. A DSSC is composed of a wide band gap semiconductor deposited on a translucent conducting substrate, an anchored molecular sensitizer, and a redox electrolyte (usually the I^-/I_3^- couple is found in most of the "conventional" DSSCs). While the total efficiency of the DSSC depends on the optimization and compatibility of each of its constituents, the initial requirement is that the photosensitizer should capture as many photons from sunlight as possible. Hence, the molecular design of a single photosensitizer with panchromatic light-harvesting characteristics is very crucial for highly efficient DSSCs. Towards this goal, a variety of panchromatic sensitizers have been investigated for applications in DSSCs. The ruthenium(II)-based panchromatic dye, coded as "black dye" (Fig. 1) has ever been developed in which the ruthenium center is coordinated to a monoprotonated tricarboxyterpyridine ligand and three thiocyanate ligands. The spectral response of the "black dye" covers the whole visible range and extends into the near-infrared (NIR) region up to 920 nm, corresponding to a power conversion efficiency (PCE) of 11.1% using a high-haze TiO_2 electrode [2]. Metallophthalocyanines (MPcs) show

* Corresponding authors. Department of Chemistry and Institute of Molecular Functional Materials, Hong Kong Baptist University, Waterloo Road, Kowloon Tong, Hong Kong, China. Fax: +852 34117348.
** Corresponding author. Fax: +81 29 859 2304.
E-mail addresses: xjzhu@hkbu.edu.hk (X. Zhu), roverqin@gmail.com (C. Qin), wywong@hkbu.edu.hk (W.-Y. Wong), wkwong@hkbu.edu.hk (W.-K. Wong).
[1] Fax: +852 34117348.
[2] Fax: +81 29 859 2304.

0143-7208/$ – see front matter © 2013 Elsevier Ltd. All rights reserved.
http://dx.doi.org/10.1016/j.dyepig.2013.11.001

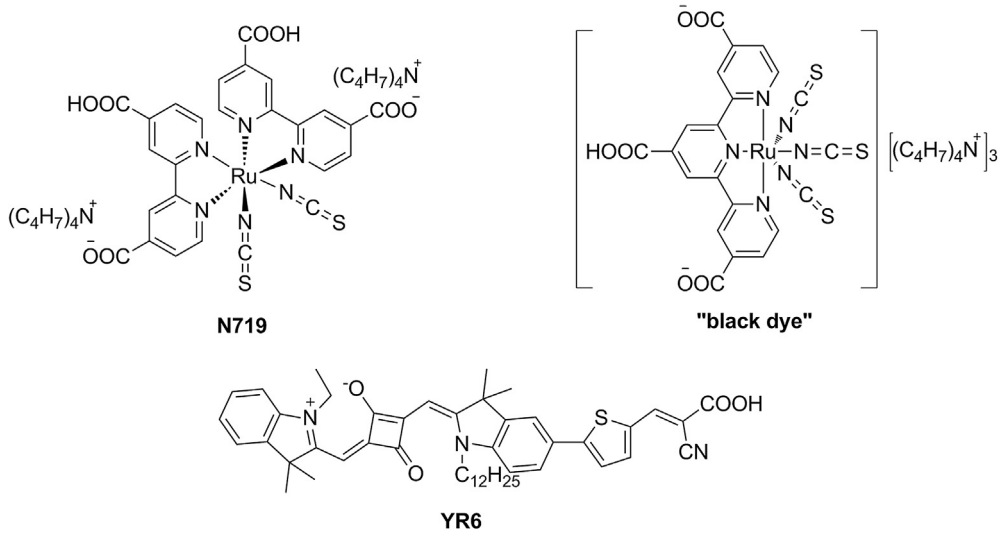

Fig. 1. Chemical structures of **N719**, **YR6** and "black dye".

potential as NIR photosensitizers because of their intense Q bands (λ = 600–700 nm), high molar extinction coefficients ($\varepsilon > 100\ 000\ M^{-1}\ cm^{-1}$), and good thermal, chemical, and photolytic stabilities [3]. However, MPc photosensitizers displayed rather low conversion efficiencies in DSSCs. The major factors for the low efficiency of MPcs were the formation of aggregates on the surface of the TiO_2 crystal and the lack of electron transfer directionality in the excited state. On the other hand, some metal-free organic photosensitizers such as squaraine [4], cyanine [5], and bodipy [6] have been applied in DSSCs for their good absorption bands in the NIR region. Specifically, squaraine-based photosensitizers absorb strongly in the NIR spectroscopic region and the most-efficient squaraine dye to date, YR6 (Fig. 1), showed a PCE of 6.7%, as well as a good incident photon-to-current conversion efficiency (IPCE >50%) in the range of 450–700 nm [7]. Recently, the strong electron acceptor benzothiadiazole unit was incorporated between donor and anchor unit to propose a novel donor–acceptor–π-spacer–acceptor (D–A–π–A) configuration for metal-free organic sensitizers. The incorporated additional acceptor of benzothiadiazole unit in the π-conjugation can improve the distribution of donor electrons to enhance the photostability of indoline compounds, and red-shift the absorption spectra into the NIR region, resulting in high PCEs [8]. Another electron-deficient unit, thiadiazolo[3,4-*c*]pyridine (PyT), has also been explored as a strong electron acceptor in the design of polymers and small molecules with relatively lower HOMO–LUMO bandgaps for efficient organic bulk heterojunction photovoltaic solar cells [9]. It has been shown that these molecules containing the PyT unit have stronger intermolecular interactions to extend their optical absorption into the NIR region to maximize photon absorption. To the best of our knowledge, organic photosensitizers based on PyT have so far not been investigated in DSSC applications.

In this article, three new organic D–A–π–A photosensitizers with PyT moiety incorporated between a non-planar triarylamine and a cyanoacrylic acid, have been developed and applied in DSSCs (Fig. 2). As expected, the spectral responses of the DSSCs based on the three dyes covered the whole visible region and reached above 800 nm (Fig. 1). Typically, different bulky triarylamine units such as triphenylamine (D1), *N*,*N*-bis(9,9-dimethylfluoren-2-yl)aniline (D2) and 4-(hexyloxy)-*N*-(4-(hexyloxy)-phenyl)-*N*-phenylaniline (D3) were utilized as donor units to investigated their influences on the photovoltaic performances of DSSCs. While the highest PCE of 4.20% is low, the methodology of tuning the HOMO or LUMO energy levels by incorporation of PyT in such D–A–π–A dyes could be generally applied to design more efficient panchromatic photosensitizers in DSSCs.

2. Experimental section

2.1. Materials and reagents

All solvents and reagents were purchased from Sigma–Aldrich Company and used as received without further purification. Optically transparent FTO-conducting glass electrodes (Nippon Sheet Glass Co., Japan) with a sheet resistance of 8–10 $\Omega\ m^{-2}$ and an optical transmission of greater than 80% in the visible-light range were used and cleaned using a standard procedure. A main transparent layer (12 μm) with titania particles (about 20 nm) and a scattering layer (4 μm) with titania particles (about 400 nm) were screen-printed onto the fluorine-doped tin oxide (FTO)-conducting glass substrate.

2.2. Instruments and characterization

^{1}H and ^{13}C NMR spectra were recorded with a Bruker Ultrashield 400 Plus NMR spectrometer. The UV–visible absorption spectra of

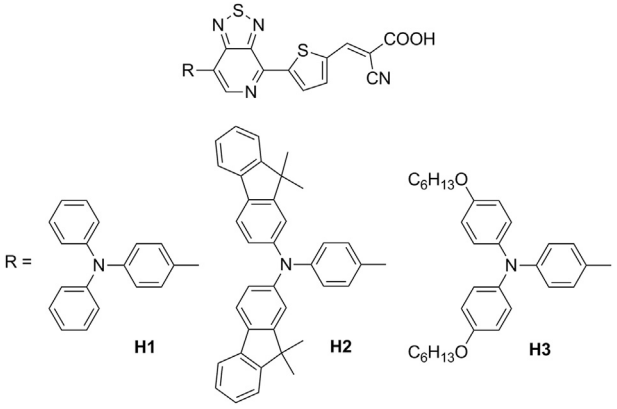

Fig. 2. Chemical structure of new dyes **H1**, **H2** and **H3**.

these dyes were measured in CH_2Cl_2 solution with a Varian Cary 100 UV–Vis spectrophotometer. High-resolution matrix-assisted laser desorption/ionization time of flight (MALDI-TOF) mass spectra were obtained with a Bruker Autoflex MALDI-TOF mass spectrometer. The cyclic voltammograms (CVs) were measured with Versastat II electrochemical work station using a normal three-electrode cell with a Pt working electrode, a Pt wire counter electrode and an Ag/Ag^+ reference electrode. The supporting electrolyte used is 0.1 M tetra-*n*-butylammonium hexafluorophosphate in CH_2Cl_2 solution. The potential of the reference electrode was calibrated by ferrocene after each set of measurements, and all potentials mentioned in the work were against normal hydrogen electrode. The photocurrent–voltage (*J*–*V*) curves of the DSSCs were measured by using a digital source meter (2400, Keithley) under standard air mass (AM 1.5) with simulated solar illumination at 100 mW cm^{-2} (WXS-90SL2, Wacom). Monochromatic incident-photon-to-current-conversion efficiency (IPCE) spectra were measured with monochromatic incident light of 1×10^{16} photons cm^{-2} in DC mode (CEP-2000 BX, Bunko-Keiki). During the *J*–*V* and IPCE measurements, a black mask and edge were used with an aperture area of 0.25 cm^2. Charge-extraction from TiO_2 was calculated by integration of the transient current that was detected when the laser illumination was turned off and the DSSCs was simultaneously stepped from open-circuit to short-circuit. Intensity-modulated photovoltage spectroscopy of the open circuit was carried out by using a combination of sinusoidal low-intensity-modulated illumination from a green diode laser (Cobolt Co., Stockholm, Sweden, Samba, 532 nm, 50 mW) band constant-bias light illumination from a Xe lamp (Ushio, Tokyo, Japan, UXL-500D-O), which was attenuated (if necessary) with a neutral-density filter. An acoustic optical modulator (Isomet Co., Springfield, VA, 1205 C-1) was used to produce sinusoidal modulation of a laser beam. Electrochemical-impedance spectroscopy (EIS) measurements of all of the DSSCs were performed on a Zahner IM6e Impedance Analyzer (ZAHNER-Elektrik GmbH &CoKG, Kronach, Germany). The frequency range was 0.1 Hz–100 kHz. The magnitude of the alternative signal was 10 mV. The applied voltage bias was −0.68 V.

2.3. Fabrication of dye-sensitized solar cells

A main transparent layer (12 μm) with titania particles (about 20 nm) and a scattering layer (4 μm) with titania particles (about 400 nm) were screen-printed onto the fluorine-doped tin oxide (FTO)-conducting glass substrate. The films were then sintered at 500 °C for 1 h. The thickness of the films was measured on a Surfcom 1400A surface profiler (Tokyo Seimitsu Co. Ltd.). The films were treated with a 0.1 M aqueous solution of HCl before examination. Coating of the titania films was carried out by immersion in a 3×10^{-4} M solution of the sensitizers in MeCN/*t*BuOH (1:1, v/v) for 24 h. The dye-covered TiO_2 electrode and the Pt counter electrode were assembled into a sandwich-type cell and sealed with a hot-melt gasket (thickness: 25 μm) that was made of the ionomer Surlyn1702 (DuPont). Finally, the electrolyte, which consisted of 0.6 M 1-methyl-3-propylimidazolium iodide (MPImI), 0.1 M LiI, 0.05 M I_2, and 0.5 M *tert*-butylpyridine in MeCN, was injected into the cell and sealed with a cover glass.

2.4. Synthesis and characterizations

2.4.1. 5-(7-Bromo-[1,2,5]thiadiazolo[3,4-c]pyridin-4-yl)thiophene-2-carbaldehyde (**1**)

The mixture of 4,7-dibromo-[1,2,5]thiadiazolo[3,4-*c*]pyridine (1.17 g, 4 mmol), (5-formylthiophen-2-yl)boronic acid (639 mg, 4.1 mmol), $Pd(PPh_3)_4$ (230 mg, 0.2 mmol) and 2 N aqueous solution of K_2CO_3 (2 mL) in THF (10 mL) under N_2 atmosphere was heated to reflux for about 48 h. Then the solvent was removed under vacuum and the residue was purified by column chromatography on silica gel using a 1:4 mixture of hexane and CH_2Cl_2 as eluent to afford the red compound. Yield: 545.8 mg, (42%). ^{1}H NMR (400 MHz, $CDCl_3$): δ (ppm) 9.87 (s, 1H), 8.64 (s, 1H), 8.52 (d, J = 1.2 Hz, 1H), 8.45 (d, J = 1.2 Hz, 1H). ^{13}C NMR (400 MHz, $CDCl_3$): δ (ppm) 190.03, 156.32, 153.52, 147.92, 145.82, 139.80, 138.19, 133.15, 126.56, 117.56. HRMS (MALDI-TOF, m/z): [M^+] calcd for ($C_{10}H_4BrN_3OS_2$) 324.8979; found, 324.8991.

2.4.2. 5-(7-(4-(Diphenylamino)phenyl)-[1,2,5]thiadiazolo[3,4-c]pyridin-4-yl)thiophene-2-carbaldehyde (**2a**)

The mixture of **1** (100 mg, 0.31 mmol), (4-(diphenylamino)-phenyl)boronic acid (116 mg, 0.4 mmol), $Pd(PPh_3)_4$ (18 mg, 0.01 mmol) and 2 N aqueous solution of K_2CO_3 (2 mL) in THF (10 mL) under N_2 atmosphere was heated to reflux for about 24 h. Then the solvent was removed under vacuum and the residue was purified by column chromatography on silica gel using a 1:3 mixture of hexane and CH_2Cl_2 as eluent to afford the dark red compound. Yield: 114 mg, (75%). ^{1}H NMR (400 MHz, $CDCl_3$): δ (ppm) 9.98 (s, 1H), 9.01 (s, 1H), 8.60 (t, J = 2.0 Hz, 2H), 8.18 (d, J = 2.0 Hz, 1H), 7.86 (d, J = 4.0 Hz, 1H), 7.30–7.35 (m, 4H), 7.19–7.22 (m, 5H), 7.17 (t, J = 2.0 Hz, 1H), 7.11–7.15 (m, 2H). ^{13}C NMR (400 MHz, $CDCl_3$): δ (ppm) 182.94, 155.29, 153.51, 152.88, 150.69, 146.77, 145.42, 143.63, 142.38, 136.80, 131.25, 129.55, 129.10, 127.90, 125.76, 124.32, 121.11, 118.66. HRMS (MALDI-TOF, m/z): [M^+] calcd for ($C_{28}H_{18}N_4OS_2$) 490.0925; found, 490.0937.

2.4.3. 5-(7-(4-(Bis(9,9-dimethyl-9H-fluoren-2-yl)amino)phenyl)-[1,2,5]thiadiazolo[3,4-c]pyridin-4-yl)thiophene-2-carbaldehyde (**2b**)

Using a similar procedure to **2a**, **2b** was separated as a purple solid. Yield: 110 mg, (71%). ^{1}H NMR (400 MHz, $CDCl_3$): δ (ppm) 9.99 (s, 1H), 9.03 (s, 1H), 8.66 (d, J = 2.0 Hz, 1H), 8.64 (d, J = 2.0 Hz, 1H), 8.20 (d, J = 4.0 Hz, 1H), 7.86 (d, J = 4.0 Hz, 1H), 7.65–7.69 (m, 4H), 7.40 (t, J = 4.0 Hz, 2H), 7.27–7.36 (m, 9H), 7.23 (t, J = 2.0 Hz, 1H), 7.21 (t, J = 2.0 Hz, 1 H), 1.25 (s, 12H). ^{13}C NMR (400 MHz, $CDCl_3$): δ (ppm) 182.95, 155.29, 153.65, 152.66, 150.91, 146.27, 143.67, 142.85, 138.74, 137.09, 135.47, 134.37, 133.97, 131.32, 129.19, 127.90, 126.87, 124.43, 122.59, 121.53, 120.82, 119.86, 119.67, 118.00, 113.84. HRMS (MALDI-TOF, m/z): [M^+] calcd for ($C_{46}H_{34}N_4OS_2$) 722.2267; found, 722.2239.

2.4.4. 5-(7-(4-(Bis(4-(hexyloxy)phenyl)amino)phenyl)-[1,2,5]thiadiazolo[3,4-c]pyridin-4-yl)thiophene-2-carbaldehyde (**2c**)

Using a similar procedure to **2a**, **2c** was obtained as a purple solid. Yield: 100 mg, (80%). ^{1}H NMR (400 MHz, $CDCl_3$): δ (ppm) 9.97 (s, 1H), 8.98 (s, 1H), 8.55 (d, J = 4.0 Hz, 2H), 8.15 (d, J = 4.0 Hz, 1H), 7.84 (d, J = 4.0 Hz, 1H), 7.13–7.15 (m, 4H), 7.00–7.02 (m, 2H), 6.86–6.88 (m, 4H), 3.95 (t, J = 6.4 Hz, 4H), 1.75–1.81 (m, 4H), 1.45–1.49 (m, 4H), 1.25–1.37 (m, 8H), 0.90 (t, J = 6.4 Hz, 6H). ^{13}C NMR (400 MHz, $CDCl_3$): δ (ppm) 182.88, 154.45, 150.59, 148.43, 141.22, 140.70, 139.68, 138.87, 134.75, 130.57, 127.74, 127.31, 126.75, 119.32, 118.94, 118.26, 116.88, 115.46, 67.64, 30.96, 28.01, 25.19, 22.00, 13.82. HRMS (MALDI-TOF, m/z): [M^+] calcd for ($C_{40}H_{42}N_4O_3S_2$) 690.2722; found, 690.2787.

2.4.5. (E)-2-Cyano-3-(5-(7-(4-(diphenylamino)phenyl)-[1,2,5]thiadiazolo[3,4-c]pyridin-4-yl)thiophen-2-yl)acrylic acid (**H1**)

A mixture of precursor **2a** (100 mg, 0.20 mmol) and cyanoacrylic acid (40 mg, 0.50 mmol) in acetic acid (20 mL) was heated under reflux in the presence of ammonium acetate (200 mg) overnight under N_2 atmosphere. Then water was added and extracted with CH_2Cl_2. Next solvent was removed under vacuum and the crude

compound was purified by column chromatography on silica gel eluting with CH_2Cl_2/MeOH (20:1, v/v) to give a purple solid. Yield: 81.0 mg (70.0%). Melting point: 254–258 °C. IR (KBr): 3446, 2966, 2931, 2859, 2221, 1668, 1591, 1487, 1433, 1327, 1263, 1189, 1109, 806. ^{1}H NMR (400 MHz, DMSO-*d*): δ (ppm) 9.15 (s, 1H), 8.53 (d, *J* = 8.8 Hz, 2H), 8.44 (s, 1H), 8.22 (d, *J* = 4.0 Hz, 1H), 8.02 (d, *J* = 4.0 Hz, 1H), 7.40 (t, *J* = 7.8 Hz, 4H), 7.16–7.21 (m, 6H), 7.02 (t, *J* = 8.8 Hz, 2H). ^{13}C NMR (400 MHz, DMSO-*d*): δ (ppm) 163.35, 154.26, 150.81, 149.76, 148.44, 146.16, 144.94, 144.23, 141.84, 138.87, 137.35, 131.02, 129.83, 128.60, 127.36, 125.54, 124.55, 120.04, 118.12, 117.06, 115.01. HRMS (MALDI-TOF, m/z): [M^+] calcd for ($C_{31}H_{19}N_5O_2S_2$) 558.1053; found, 558.1030.

2.4.6. (E)-3-(5-(7-(4-(Bis(9,9-dimethyl-9H-fluoren-2-yl)amino) phenyl)-[1,2,5]thiadiazolo[3,4-c]pyridin-4-yl)thiophen-2-yl)-2-cyanoacrylic acid (*H2*)

Using a similar procedure as for **H1**, **H2** was separated as a dark-purple solid. Yield: 70 mg, (65.2%). Melting point: 225–230 °C. IR (KBr): 3446, 2966, 2924, 2859, 2221, 1625, 1593, 1455, 1431, 1313, 1266, 1186, 1110, 807. δ (ppm) ^{1}H NMR (400 MHz, DMSO-*d*): δ (ppm) 9.10 (s, 1H), 8.56 (d, *J* = 8.4 Hz, 2H), 8.25 (s, 1H), 8.18 (d, *J* = 3.6 Hz, 1H), 7.88 (d, *J* = 3.6 Hz, 1H), 7.72–7.78 (m, 4H), 7.48 (d, *J* = 7.2 Hz, 2H), 7.36 (d, *J* = 7.2 Hz, 2H), 7.24–7.32 (m, 4H), 7.11–7.17 (m, 4H), 1.36 (s, 12H). ^{13}C NMR (400 MHz, DMSO-*d*): δ (ppm) 163.22, 154.94, 154.30, 153.25, 150.44, 149.77, 148.47, 145.73, 144.81, 142.37, 141.46, 139.61, 138.04, 136.84, 134.91, 130.97, 128.94, 128.08, 127.42, 127.10, 126.95, 124.16, 122.70, 121.27, 120.75, 119.75, 119.60, 118.37, 118.19, 46.52, 26.64. HRMS (MALDI-TOF, m/z): [M^+] calcd for ($C_{49}H_{35}N_5O_2S_2$) 790.2305; found, 790.2274.

2.4.7. (E)-3-(5-(7-(4-(Bis(4-(hexyloxy)phenyl)amino)phenyl)-[1,2,5]thiadiazolo[3,4-c]pyridin-4-yl)thiophen-2-yl)-2-cyanoacrylic acid (*H3*)

Using a similar procedure as for **H1**, **H3** was obtained as a dark-purple solid. Yield: 82 mg, (69.7%). Melting point: 161–165 °C. IR (KBr): 3445, 2956, 2924, 2860, 2221, 1668, 1591, 1502, 1465, 1318, 1242, 1190, 1109, 826. δ (ppm) ^{1}H NMR (400 MHz, DMSO-*d*): δ (ppm) 9.07 (s, 1H), 8.51 (d, *J* = 7.2 Hz, 2H), 8.17 (d, *J* = 4.0 Hz, 1H), 8.12 (s, 1H), 7.81 (d, *J* = 4.0 Hz, 1H), 7.13 (d, *J* = 8.8 Hz, 4H), 6.95 (d, *J* = 8.8 Hz, 4H), 6.84 (d, *J* = 8.8 Hz, 2H), 3.96 (t, *J* = 6.4 Hz, 4H), 1.68–1.75 (m, 4H), 1.39–1.46 (m, 4H), 1.23–1.39 (m, 8H), 0.90 (t, *J* = 6.4 Hz, 6H). ^{13}C NMR (400 MHz, DMSO-*d*): δ (ppm) 156.07, 154.40, 150.68, 150.51, 148.49, 141.29, 140.70, 139.65, 138.71, 138.67, 134.78, 130.87, 127.74, 127.23, 126.76, 119.33, 118.92, 118.19, 116.91, 115.59, 110.87, 67.64, 30.97, 28.66, 25.18, 22.05, 13.88. HRMS (MALDI-TOF, m/z): [M^+] calcd for ($C_{43}H_{43}N_5O_4S_2$) 758.2829; found, 758.2814.

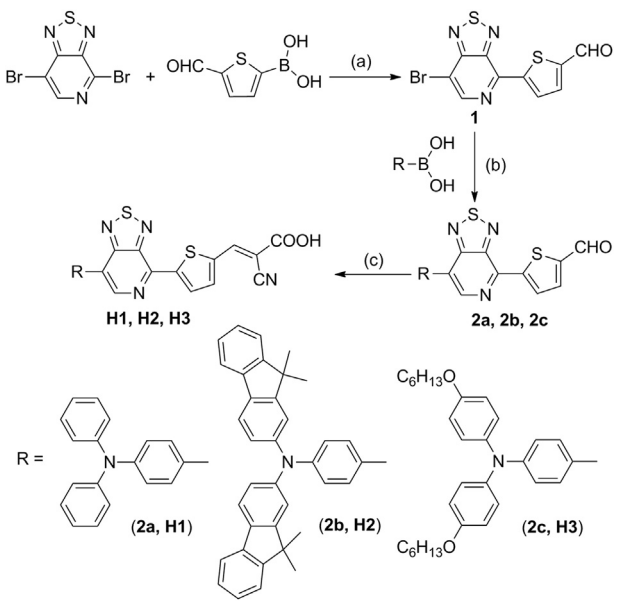

Scheme 1. Synthetic routes for the dyes **H1**, **H2** and **H3**. Reaction conditions: (a) $Pd(PPh_3)_4$, K_2CO_3 (2 N), THF/reflux; (b) $Pd(PPh_3)_4$, K_2CO_3 (2 N), THF, reflux; (c) $CNCH_2COOH$, CH_3COOH, CH_3COONH_4, reflux.

3. Results and discussion

3.1. Synthesis and characterization

The synthetic procedures of the three dyes are depicted in Scheme 1. The key precursors to 4,7-dibromo-[1,2,5]thiadiazolo-[3,4-*c*]pyridine [9a], (4-(diphenylamino) phenyl)boronic acid, (4-(bis(9,9-dimethyl-9*H*-fluoren-2-yl)-amino)phenyl)boronic acid and (4-(bis(4-(hexyloxy)phenyl)amino)phenyl)boronic acid were synthesized according to the literature methods [10]. Compounds **1**, **2a**, **2b** and **2c** were prepared through conventional Suzuki cross-coupling reaction in good yield and the three target photosensitizers (**H1**, **H2, H3**) were separated after typical Knoevenagel reactions between the cyanoacrylic acid and the formylated intermediates. All the new compounds were characterized by ^{1}H NMR and ^{13}C NMR spectroscopy and MALDI-TOF mass spectrometry.

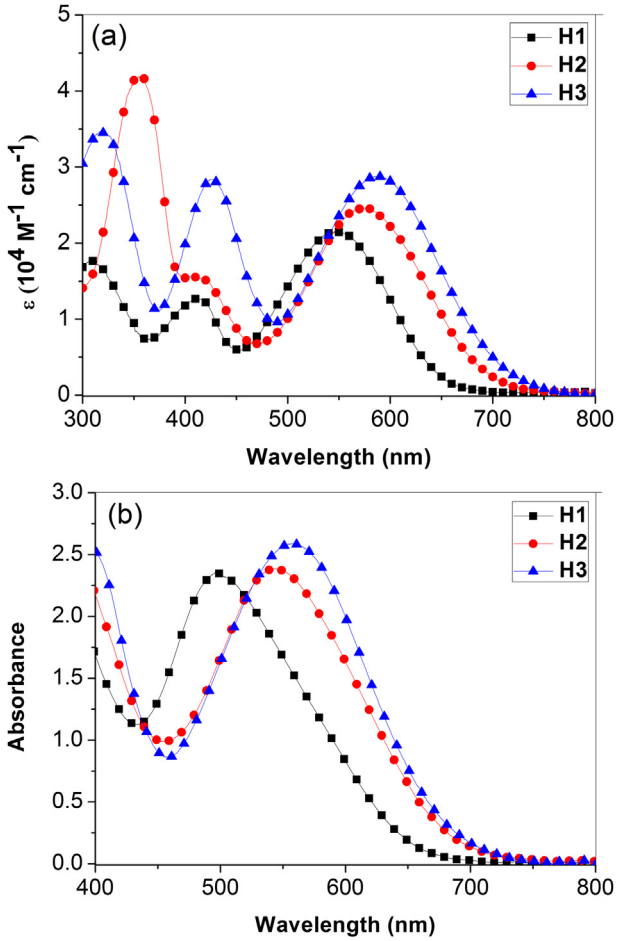

Fig. 3. Absorption spectra of dyes (a) in CH_2Cl_2 solution and (b) on TiO_2 films.

3.2. UV–visible absorption properties

The optical absorption spectra of three new dyes **H1**, **H2** and **H3** in dichloromethane solutions and adsorbed on TiO_2 films are shown in Fig. 3, and the corresponding spectroscopic data are summarized in Table 1. The three dyes exhibited similar broad and strong absorption spectra covering a wide wavelength range of 300–750 nm (Fig. 3). The shorter wavelength region corresponds to the π–π* transitions of the conjugated system and the longer wavelength region can be reasonably assigned to the efficient intramolecular charge transfer (ICT) between the donor and the acceptor. As expected, the introduction of PyT unit into the molecular frame distinctly exhibits broad and efficient optical absorption above 750 nm to maximize photon absorption. Obviously, in the three photosensitizers containing the same cyanoacetic acid unit, the ICT band is dependent upon the donor units and electron transport channels. As listed in Table 1, the donor effect on absorption peak is distinct. A bathochromic shift of 29 and 39 nm was observed by replacing D1 (**H1**) with D2 (**H2**) and D3 unit (**H3**) in the donor moiety, respectively. This definitely indicates that that the electron-donating capability is in the order of D3 > D2 > D1, which is consistent with the electrochemical properties (*vide infra*). In addition, the corresponding molar extinction coefficients of ICT peaks are in the order of H3 (585 nm, 2.87×10^4 M^{-1} cm^{-1}) > H2 (575 nm, 2.46×10^4 M^{-1} cm^{-1}) > H1 (546 nm, 2.14×10^4 M^{-1} cm^{-1}). The results clearly illustrate that the introduction of D3 donor group in **H3** is favorable for lowering the band gap and extending the responsive wavelength to nearly 800 nm, as well as capturing more solar light for a higher photocurrent output. When adsorbed on a transparent thin TiO_2 film, the three dyes showed broad absorption spectra in agreement with those in solutions (Fig. 3(b)), while the ICT absorption peaks displayed a slight blue-shift of 49, 31, and 27 nm for **H1**, **H2**, and **H3**, respectively. Such a hypsochromic shift is mainly due to the deprotonation and H-aggregation between the carboxylate acid and the TiO_2 semiconductor [11]. Notably, the maximum absorption band of **H3** is less blue-shifted than that of **H1** and **H2**, indicating that the introduction of hexyloxy chain on the triarylamine moiety effectively inhibits H-aggregation.

3.3. Electrochemical properties

To evaluate the possibility of photoelectron injection and sensitizer regeneration, the cyclic voltammograms have been performed in CH_2Cl_2 solution with ferrocene (0.4 V vs. NHE) as an external reference. The voltammograms of the three dyes (Fig. 4) showed symmetrical and reversible behavior, indicative of high redox stability. The oxidation potentials correspond to the highest occupied molecular orbitals (HOMO), which are exclusively determined by the donors. As listed in Table 1, the HOMO levels of the three dyes are in the order of **H1** (0.86 V) > **H2** (0.64 V) > **H3** (0.57 V). It can be rationalized that the donor groups with increasing electron-donating capability decrease the HOMO energy in the same order. Obviously, the HOMO values of the three dyes are more positive than I^-/I_3^- redox potential value (0.4 V), indicating that the oxidized dyes can be efficiently regenerated by the electrolyte. The lowest unoccupied molecular orbitals (LUMO) can be calculated by the values of E_{ox} and the zero–zero bandgaps (E_{0-0}) determined from the onset of the UV–visible absorption spectra. The estimated E_{0-0} is 1.99 eV, 1.78 eV and 1.72 eV for **H1**, **H2** and **H3,** respectively. The values of the HOMO-LUMO bandgap for the three dyes are relatively low, indicating that the incorporation of PyT can effectively decrease the energy bandgap and extend the absorption spectrum. Subsequently, the LUMO values of the three dyes, calculated from $E_{HOMO}-E_{0-0}$ are −1.13, −1.14 V and −1.15 V for **H1**, **H2** and **H3**, respectively, which are more negative than the conduction band edge (CB) of TiO_2 (−0.5 V vs. NHE), allowing the efficient electron injection from the oxidized organic dyes into the conduction band of TiO_2.

Table 1
Photophysical and electrochemical properties of the three organic dyes.

Dye	λ_{max} [nm][a] ($\varepsilon/10^4$ M^{-1} cm^{-1})	λ_{max} [nm][b]	E_{ox} [V][c]	E_{0-0} [eV][d]	E^*_{ox} [V][e]
H1	546 (2.14)	497	0.86	1.99	−1.13
H2	575 (2.46)	544	0.64	1.78	−1.14
H3	585 (2.87)	558	0.57	1.72	−1.15

[a] Absorption maximum in 1×10^{-5} mol L^{-1} CH_2Cl_2 solution.
[b] Absorption maximum on TiO_2 film.
[c] Oxidation potential in CH_2Cl_2 solution containing 0.1 M $(n\text{-}C_4H_9)_4NPF_6$ with a scan rate 100 mV s^{-1} (*vs.* NHE).
[d] E_{0-0} was determined from the onset of absorption spectra.
[e] $E^*_{ox} = E_{ox} - E_{0-0}$.

3.4. Theoretical calculations

To understand the geometrical and electronic properties of these dyes, density functional theory (DFT) calculations are performed using Gaussian 03 program package at the B3LYP/6-31 G(d) level. The electron distributions of the HOMOs and LUMOs of these dyes are shown in Fig. 5. It was found that HOMOs of the three dyes are distributed mainly over the entire triarylamine donor part, while the LUMOs are mainly delocalized over cyanoacrylic acid, thiophene conjugated spacer and PyT acceptor. Generally, the HOMO orbitals are delocalized through the donor and π-bridge in traditional D–π–A type of dyes. However, in our D–A–π–A structural dyes, this connection might be somewhat blocked from the electron-withdrawing unit PyT in the bridge. Initially, in designing dyes of D–A–π–A configuration, the electrons on the donor subunit are not directly transferred to the cyanoacetic acid subunit during the photo-excitation, but successively transferred to the electron-trap PyT subunit, then to the cyanoacetic acid subunit, and finally to TiO_2. Here, the insufficient overlap of the HOMO and LUMO orbitals implies that the strong acceptor PyT may retard a fast charge transition from the donor to the anchor group, which is partly ascribed to the relatively low PCE based on the three dyes, regardless of their panchromatic light response.

3.5. Photovoltaic performance

Fig. 6 shows the IPCE spectra of DSSCs based on the three dyes as a function of light excitation wavelength. Notably, these DSSCs

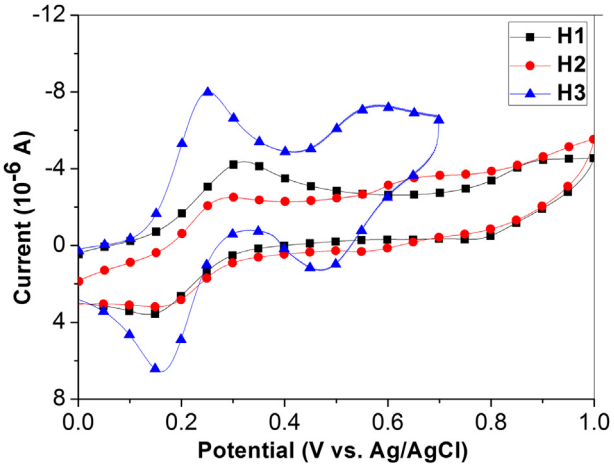

Fig. 4. Cyclic voltammograms of dyes **H1**–**H3** in CH_2Cl_2 solution.

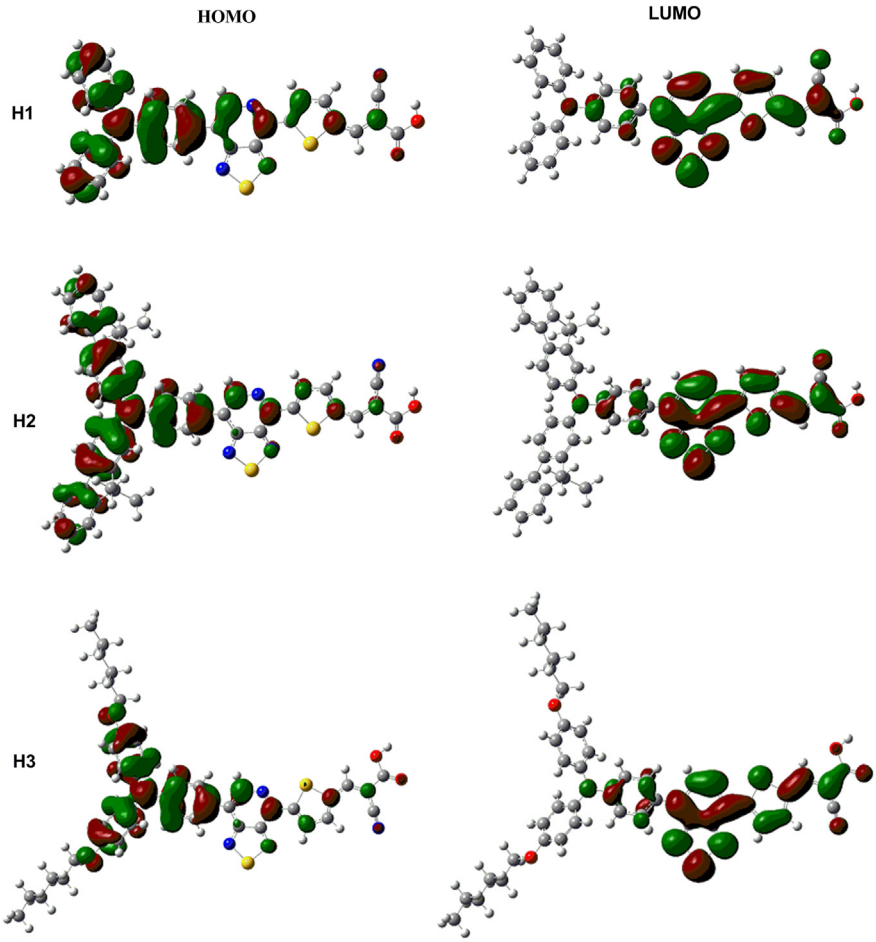

Fig. 5. Frontier molecular orbitals of the HOMO and LUMO (right) calculated by DFT on a B3LYP/6-31 G (d)* level.

exhibited remarkably broad IPCE spectra covering the whole visible region with the threshold wavelength over 800 nm, which matched well with the threshold wavelength of the absorption spectra when adsorbed onto TiO_2 films. It means that incorporation of PyT unit in the three dyes with good delocalization between the donor and the acceptor can broaden the absorption spectrum to get a broad IPCE. From the IPCE curves, the IPCE exceeded 50% in the spectral range of 300–650 nm for the three photosensitizers, and the solar cells based on **H3** showed the highest IPCE value of 65% at 583 nm. These results also indicate that **H3** dye possesses better light-harvesting ability and would generate a higher photocurrent among the three dyes.

The photocurrent–voltage (J–V) characteristics of all devices are shown in Fig. 7. The parameters of DSSCs fabricated with these dyes, i.e., short-circuit current (J_{sc}), open-circuit photovoltage (V_{oc}), fill factor (FF), and total power conversion efficiency (η), are

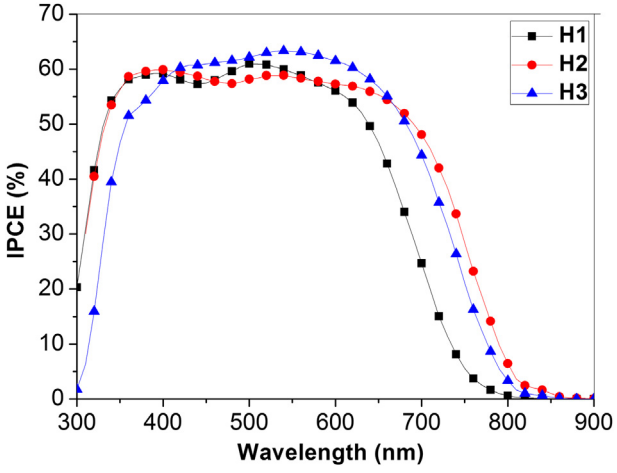

Fig. 6. IPCE curves of organic dyes **H1**–**H3**.

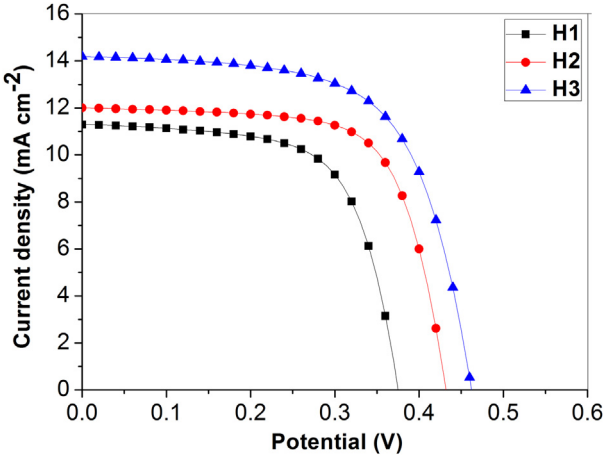

Fig. 7. The photocurrent-voltage (J–V) curves of DSSCs.

Table 2
Photovoltaic parameters of the dyes in liquid based DSSCs at full sunlight (AM 1.5G, 100 mW cm^{-2}).

Dye	J_{sc} [mA cm^{-2}]	V_{oc} [V]	FF	η [%]
H1	11.23	0.367	0.64	2.63
H2	12.00	0.432	0.69	3.58
H3	14.19	0.462	0.64	4.20

summarized in Table 2. DSSC based on dye **H3** shows the highest PCE of 4.20% with a relatively higher J_{sc} = 14.19 mA cm^{-2}, V_{oc} = 0.462 V, and FF = 0.64 under AM 1.5 irradiation. And the dyes **H1** and **H2** sensitized solar cells displayed relatively inferior photovoltaic performance (η) of 2.63% and 3.58% due to the lower J_{sc} and V_{oc}. Compared with dyes **H1** and **H2**, the significant improvement of photovoltaic performances for **H3** should be attributed to the more efficient light harvesting, effective electron injection and slower charge recombination rate (*vide infra*). For example, the LUMO energy levels of the three dyes are in the order of **H3** (−1.15 V) < **H2** (−1.14 V) < **H1** (−1.13 V), indicating that DSSC based on **H3** exhibited the most effective electron injection from the excited dye into the CB of TiO_2. As a result, DSSC based on **H3** showed the highest V_{oc} and J_{sc} due to its better molar extinction coefficient, broad IPCE curve and high electron-injection efficiency. In addition, D3 appended with a long hexyloxy chain in **H3** can effectively suppress dye-aggregation and retard charge recombination in DSSC (*vide infra*) [12].

3.6. Electrochemical Impedance Spectroscopy

Electrochemical Impedance Spectroscopy (EIS) has been performed to elucidate the interfacial charge recombination process in DSSCs based on these dyes under the dark condition. As shown in Fig. 8, a major semicircle for each dye was observed in the EIS Nyquist plot, which is related to the resistance of electron transport at the TiO_2/dye/electrolyte interface, i.e., the resistance of the recombination between electrons on TiO_2 conduction band and I_3^- species in the electrolyte [13]. The larger the semicircle, the slower the recombination kinetics. It is clear that dye **H3** exhibited the highest recombination resistance, which is most likely due to the long hexyloxy chain on D3 that more efficiently closes up the area for direct contact between TiO_2 and the electrolytes [10]. A high V_{oc} is related to a low rate of charge recombination. The trend observed is definitely consistent with the V_{oc} values of the cells. As for dye **H3**, the introduction of a bulky electron-donating unit D3 appended with long hexyloxy chain can not only further extend absorption spectrum, but also efficiently provide a surface blocking layer on the TiO_2 surface and impede a direct contact between the charge and oxidized species (I_3^-) in the electrolyte [10].

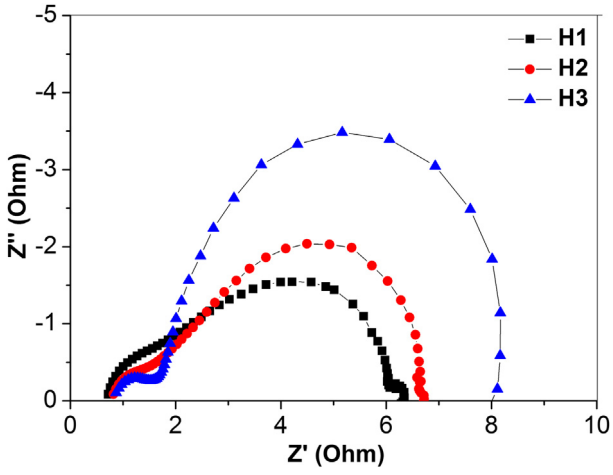

Fig. 8. EIS Nyquist plots for DSSCs based on the dyes under dark.

4. Conclusions

In conclusion, three new D–A–π–A photosensitizers incorporating with electron-withdrawing unit PyT as an additional acceptor have been synthesized and applied in DSSCs. It has been demonstrated that the incorporation of the PyT unit can effectively tune the HOMO and LUMO energy levels and extend the absorption spectra into deep red region by decreasing the energy bandgap. As expected, the photoresponse of DSSCs based on the three dyes covered the whole visible region and reached above 800 nm, which are comparable to the incident IPCE onset of N719. Specifically for dye **H3**, the introduction of a bulky electron-donating unit D3 appended with hexyloxy chain results in a further red-shift of the ICT band and an enhanced light-harvesting property, as well as a retarded electron recombination between the charge and oxidized species (I_3^-) in the electrolyte. Though the conversion efficiency of 4.20% is still low, the approach of tuning the HOMO or LUMO energy level by incorporation of electron-withdrawing PyT unit in such D–A–π–A dyes could be generally applied in the design of more efficient panchromatic photosensitizers in DSSCs.

Acknowledgments

We thank the National Natural Science Foundation of China (NSFC) (91222201), Hong Kong Research Grants Council (HKBU202210, HKBU202811, HKBU203011 and HKUST2/CRF/10) and Hong Kong Baptist University (FRG2/12-13/050, FRG2/11-12/007) for financial support. W.-K.W. and W.-Y.W. also thank a grant from Areas of Excellence Scheme, University Grants Committee, Hong Kong (Project No. [AoE/P-03/08]). W.-Y.W. also thanks the National Basic Research Program of China (973 Program: grant number 2013CB834702) for financial support. C. J. and L. H. thank financial supports from Core Research for Evolutional Science and Technology (CREST) of the Japan Science and Technology Agency.

References

[1] a) O'Regan B, Grätzel M. A low-cost, high-efficiency solar cell based on dye-sensitized colloidal TiO_2 films. Nature 1991;353:737–40;
b) Nazeeruddin MK, Kay IRA, Humphry-Baker R, Mueller E, Liska P, Vlachopoulos N, et al. Conversion of light to electricity by cis-XzBis(2,2'-bipyridyl-4,4'-dicarboxylate)ruthenium(II) charge-transfer sensitizers (X = C1–, Br–, I–, CN–, and SCN–) on nanocrystalline TiO_2 electrodes. J Am Chem Soc 1993;115:6382–90;
c) Nazeeruddin MK, Splivallo R, Liska P, Comte P, Grätzel M. A swift dye uptake procedure for dye sensitized solar cells. Chem Commun 2003;12:1456–7;
d) Nazeeruddin MK, Péchy P, Grätzel M. Efficient panchromatic sensitization of nanocrystalline TiO_2 films by a black dye based on atrithiocyanato–ruthenium complex. Chem Commun 1997;18:1705–6;
e) Han LY, Islam A, Chen H, Malapaka C, Chiranjeevi B, Zhang SF, et al. High-efficiency dye-sensitized solar cell with a novel co-adsorbent. Energy Environ Sci 2012;5:6057–60.

[2] a) Numata Y, Singh SP, Islam A, Iwamura M, Imai A, Nozaki K, et al. Enhanced light-harvesting capability of a panchromatic Ru(II) sensitizer based on π-extended terpyridine with a 4-methylstylryl group for dye-sensitized solar cells. Adv Funct Mater 2013;23:1817–23;
b) Liu SH, Fu HS, Cheng YM, Wu KL, Ho ST, Chi Y, et al. Theoretical study of N749 dyes anchoring on the (TiO_2)28 surface in DSSCs and their electronic absorption properties. J Phys Chem C 2012;116:16338–45;
c) Nazeeruddin MK, Pechy P, Renouard T, Zakeeruddin SM, Humphry-Baker R, Comte P, et al. Engineering of efficient panchromatic sensitizers for nanocrystalline TiO_2-based solar cells. J Am Chem Soc 2001;123:1613–24.

[3] a) Paek S, Choi H, Kim C, Cho N, So S, Song K, et al. Efficient and stable panchromatic squaraine dyes for dye-sensitized solar cells. Chem Commun 2011;47:2874–6;
b) Robertson N. Catching the rainbow: light harvesting in dye-sensitized solar cells. Angew Chem Int Ed 2008;47:1012–4;

c) He JJ, Benko G, Korodi F, Polivka T, Lomoth R, Akermark B, et al. Modified phthalocyanines for efficient near-IR sensitization of nanostructured TiO_2 electrode. J Am Chem Soc 2002;124:4922–32;
d) Kimura M, Nomoto H, Masaki N, Mori S. Dye molecules for simple co-sensitization process: fabrication of mixed-dye-sensitized solar cells. Angew Chem Int Ed 2012;51(18):4371–4;
e) Ragoussi ME, Cid JJ, Yum JH, Torre G, Censo DD, Grätzel M, et al. Carboxyethynyl anchoring ligands: a means to improving the efficiency of phthalocyanine-sensitized solar cells. Angew Chem Int Ed 2012;52(18):4375–9.

[4] a) Li JY, Chen CY, Ho WC, Chen SH, Wu CG. Unsymmetrical squaraines incorporating quinoline for near infrared responsive dye-sensitized solar cells. Org Lett 2012;14(21):5420–3;
b) Kim S, Mor GK, Paulose M, Varghese OK, Baik C, Grimes CA. Molecular design of near-IR harvesting unsymmetrical squaraine dyes. Langmuir 2010;26(16):13486–92;
c) Yum JH, Walter P, Huber S, Rentsch D, Geiger T, Nuesch F, et al. Efficient far red sensitization of nanocrystalline TiO_2 flms by an unsymmetrical squaraine dye. J Am Chem Soc 2007;129(34):10320–1.

[5] Sudeep PK, Takechi K, Kamat PV. Harvesting photons in the infrared. electron injection from excited tricarbocyanine dye (IR-125) into TiO_2 and Ag@TiO_2 core–shell nanoparticles. J Phys Chem C 2007;111(1):488–94.

[6] Kolemen S, Bozdemir OA, Cakmak Y, Barin G, Erten-Ela S, Marszalek M, et al. Optimization of distyryl-bodipy chromophores for efficient panchromatic sensitization in dye sensitized solar cells. Chem Sci 2011;2:949–54.

[7] a) Kimura M, Masuo J, Tohata Y, Obuchi K, Masaki N, Murakami TN, et al. Improvement of TiO_2/dye/electrolyte interface conditions by positional change of alkyl chains in modified panchromatic Ru complex dyes. Chem Eur J 2013;19(3):1028–34;
b) Qin C, Wong W-Y, Han L. Squaraine dyes for dye-sensitized solar cells: recent advances and future challenges. Chem Asian J 2013;8(8):1706–19.

[8] a) Wu YZ, Zhu WH. Organic sensitizers from D–π–A to D–A–π–A: effect of the internal electron-withdrawing units on molecular absorption, energy levels and photovoltaic performances. Chem Soc Rev 2013;42:2039–58;
b) Wu YZ, Zhang X, Li WQ, Wang ZS, Tian H, Zhu WH. Hexylthiophene-featured D–A–π–A structural indoline chromophores for coadsorbent-free and panchromatic dye-sensitized solar cells. Adv Energy Mater 2012;2(1):149–56;
c) Haid S, Marszalek M, Mishra A, Wielopolski M, Teuscher J, Moser JE, et al. Significant improvement of dye-sensitized solar cell performance by small structural modification in π-conjugated donor–acceptor dyes. Adv Funct Mater 2012;22(6):1291–302;
d) Lin RYY, Lee CP, Chen YC, Peng JD, Chu TC, Chou HH, et al. Benzothiadiazole-containing donor–acceptor–acceptor type organic sensitizers for solar cells with ZnO photoanodes. Chem Commun 2012;48:12071–3.

[9] a) Sun Y, Chien SC, Yip HL, Zhang Y, Chen KS, Zeigler DF, et al. High-mobility low-bandgap conjugated copolymers based on indacenodithiophene and thiadiazolo[3,4-*c*]pyridine units for thin film transistor and photovoltaic applications. J Mater Chem 2011;21:13247–55;
b) Blouin N, Michaud A, Gendron D, Wakim S, Blair E, Neagu-Plesu R, et al. Toward a rational design of poly(2,7-carbazole) derivatives for solar cells. J Am Chem Soc 2008;130(2):732–42;
c) Welch GC, Perez LA, Hoven CV, Zhang Y, Dang XD, Sharenko A, et al. A modular molecular framework for utility in small-molecule solution-processed organic photovoltaic devices. J Mater Chem 2011;21:12700–9;
d) Zhou HX, Yang LQ, Price SC, Knight KJ, You W. Enhanced photovoltaic performance of low-bandgap polymers with deep LUMO levels. Angew Chem Int Ed 2010;49(43):7992–5;
e) Steinberger S, Mishra A, Reinold E, Levichkov J, Uhrich C, Pfeiffer M, et al. Vacuum-processed small molecule solar cells based on terminal acceptor-substituted low-band gap oligothiophenes. Chem Commun 2011;47:1982–4;
f) Welch GC, Bazan GC. Lewis acid adducts of narrow band gap conjugated polymers. J Am Chem Soc 2011;133(12):4632–44;
g) Ying L, Hsu BBY, Zhan HM, Welch GC, Zalar P, Perez LA, et al. Regioregular pyridal[2,1,3]thiadiazole π-conjugated copolymers. J Am Chem Soc 2011;133:18538–41.

[10] Hua Y, Jin B, Wang HD, Zhu XJ, Wu WJ, Cheung MS, et al. New phenothiazine-based dyes for efficient dye-sensitized solar cells:positioning effect of a donor group on the cell performance. J Power Sources 2013;237:195–203.

[11] a) Mao JY, Gao FL, Ying WJ, Wu WJ, Li J, Hua JL. Benzotriazole-bridged sensitizers containing a furan moiety for dye-sensitized solar cells with high open-circuit voltage performance. Chem Asian J 2012;7(5):982–91;
b) Hua Y, Chang S, Huang DD, Zhou X, Zhu XJ, Zhao JZ, et al. Significant improvement of dye-sensitized solar cell performance using simple phenothiazine-based dyes. Chem Mater 2013;25(10):2146–53.

[12] a) Kim S, Kim D, Choi H, Kang MS, Song K, Kang SO, et al. Enhanced photovoltaic performance and long-term stability of quasi-solid-state dye-sensitized solar cells *via* molecular engineering. Chem Commun 2008;40:4951–3;
b) Qin C, Islam A, Han L. Incorporating a stable fluorenone unit into D–A–π–A organic dyes for dye-sensitized solar cells. J Mater Chem 2012;22:19236–43.

[13] a) Dai FR, Chen YC, Lai LF, Wu WJ, Cui CH, Tan GP, et al. Unsymmetric platinum(II) bis(aryleneethynylene) complexes as photosensitizers for dye-sensitized solar cells. Chem Asian J 2012;7(6):1426–34;
b) Shi J, Chen JN, Chai ZF, Wang H, Tang RL, Fan K, et al. High performance organic sensitizers based on 11,12-bis(hexyloxy) dibenzo[*a*,*c*]phenazine for dye-sensitized solar cells. J Mater Chem 2012;22:18830–8.